Journal of Visualized Experiments

Laser-Induced Fluorescence Emission (L.I.F.E.) as Novel Non-Invasive Tool for In-Situ Measurements of Biomarkers in Cryospheric Habitats

--Manuscript Draft--

Article Type:	Invited Methods Article - Author Produced Video
Manuscript Number:	JoVE60447R2
Full Title:	Laser-Induced Fluorescence Emission (L.I.F.E.) as Novel Non-Invasive Tool for In-Situ Measurements of Biomarkers in Cryospheric Habitats
Section/Category:	JoVE Environment
Keywords:	LASER-INDUCED FLUORESCENCE EMISSION (L.I.F.E.), NON-INVASIVE, CRYOSPHERIC HABITATS, ICE, PHYCOERYTHRIN, CHLOROPHYLL, GLACIAL MELT, SUPRAGLACIAL HABITATS, CRYOCONITE HOLES, CLIMATE CHANGE
Corresponding Author:	Birgit Sattler, PhD. Universität Innsbruck Innsbruck, AUSTRIA
Corresponding Author's Institution:	Universität Innsbruck
Corresponding Author E-Mail:	Birgit.Sattler@uibk.ac.at
Order of Authors:	Klemens Weisleitner
	Lars Hunger
	Christoph Kohstall
	Albert Frisch
	Michael C. Storrie-Lombardi
	Birgit Sattler, PhD.
Additional Information:	
Question	**Response**
Please indicate whether this article will be Standard Access or Open Access.	Open Access (US$3000)

TITLE:

Laser-Induced Fluorescence Emission (L.I.F.E.) as Novel Non-Invasive Tool for In-Situ Measurements of Biomarkers in Cryospheric Habitats

AUTHORS AND AFFILIATIONS:

Klemens Weisleitner[1,2], Lars Hunger[3], Christoph Kohstall[4], Albert Frisch[5], Michael C. Storrie-Lombardi[6], Birgit Sattler[1,2]

[1]Institute of Ecology, University of Innsbruck, Innsbruck, Austria
[2]Austrian Polar Research Institute, University of Vienna, Vienna, Austria
[3]BrainLinks-BrainTools, Bernstein Center Freiburg, Freiburg, Germany
[4]Stanford University, Atom Science, Kasevich Lab, Stanford, CA, USA
[5]University of Innsbruck, Institute of Experimental Physics, Innsbruck, Austria
[6]Harvey Mudd College, Department of Physics, Extraterrestrial Vehicle Instruments Laboratory, Claremont, CA, USA

Corresponding Author:

Birgit Sattler (birgit.sattler@uibk.ac.at)

Email Addresses of Co-authors:

Klemens Weisleitner (klemens.weisleitner@uibk.ac.at)
Lars Hunger (lars.hunger@brainlinks-braintools.uni-freiburg.de)
Christoph Kohstall (christoph.kohstall@gmail.com)
Albert Frisch (albert.frisch@catbull.com)
Michael C. Storrie-Lombardi (mstorrielombardi@g.hmc.edu)

KEYWORDS:

laser-induced fluorescence emission (L.I.F.E.), non-invasive, cryospheric habitats, ice, phycoerythrin, chlorophyll, glacial melt

SUMMARY:

Carbon fluxes in the cryosphere are hardly assessed yet but are crucial regarding climate change. Here we show a novel prototype device that captures the phototrophic potential in supraglacial environments based on laser-induced fluorescence emission (L.I.F.E.) technology offering high spectral and spatial resolution data under in situ conditions.

ABSTRACT:

Global warming affects microbial communities in a variety of ecosystems, especially cryospheric habitats. However, little is known about microbial-mediated carbon fluxes in extreme environments. Hence, the methodology of sample acquisition described in the very few studies available implies two major problems: A) high resolution data require a large number of samples, which is difficult to obtain in remote areas; B) unavoidable sample manipulation such as cutting, sawing, and melting of ice cores that leads to a misunderstanding of in situ conditions. In this study, a prototype device that requires neither sample preparation nor sample destruction is presented. The device can be used for in situ measurements with a high spectral and spatial resolution in terrestrial and ice ecosystems and is based on the **L**aser-**I**nduced **F**luorescence **E**mission (**L.I.F.E.**) technique. Photoautotrophic supraglacial communities can be identified by the detection of L.I.F.E. signatures in

photopigments. The L.I.F.E. instrument calibration for the porphyrin derivates chlorophyll$_a$ (chl$_a$) (405 nm laser excitation) and B-phycoerythrin (B-PE) (532 nm laser excitation) is demonstrated. For the validation of this methodology, L.I.F.E. data were ratified by a conventional method for chl$_a$ quantification that involved pigment extraction and subsequent absorption spectroscopy. The prototype applicability in the field was proven in extreme polar environments. Further testing on terrestrial habitats took place during Mars analog simulations in the Moroccan dessert and on an Austrian rock glacier. The L.I.F.E. instrument enables high resolution scans of large areas with acceptable operation logistics and contributes to a better understanding of the ecological potential of supraglacial communities in the context of global change.

INTRODUCTION:

The cryosphere harbors sea ice, glaciers, high mountain lakes, snow areas, lake ice, melt water streams, and permafrost. These areas cover approximately 11% of the earth's landmasses[1,2] and are overarched by the atmosphere as a recognized cryospheric environment. Recent studies show that massive areas of the cryosphere are quickly retreating[3,4]. The Antarctic[5,6], the Alps[7], the Arctic[8], and other regions show negative ice mass balances. The retreat of ice caps and glaciers leads to the depletion of our largest freshwater reservoir on Earth. In some areas, glacier retreat is unstoppable[5].

For a long time, ice ecosystems were considered sterile environments. However, despite harsh conditions, the presence of active life in the earth's cryosphere is evident[9-15]. Due to the trend towards massive losses of ice by melting, the cryosphere is going through a shift in biological activity, affecting adjacent habitats. To understand those partially irreversible changes we require methods to investigate biological activity in ice under in situ conditions with high spatial and temporal resolution.

In supraglacial environments, life can be found in cryoconite holes, snow covers, melted water, streams, and on bare ice surfaces. However, the most obvious supraglacial habitats are cryoconite holes. They appear globally in glaciated environments and were first described by the Swedish explorer Adolf Erik Nordenskjold during an expedition to Greenland in the 1870's[16,17]. The name originates from the Greek words "kryos" (cold) and "konia" (dust). Aeolian-derived dark organic and inorganic debris attach on the ice surface and reduce the albedo locally. Solar radiation promotes melting of the debris into deeper ice layers, forming cylindrical basins with sediment (cryoconite) in the bottom[9]. Cryoconite holes cover 0.1–10% of glacial ablation zones[11].

Cryoconite communities consist of viruses, fungi, bacteria, cyanobacteria, microalgae, and protozoa. Depending on the region, metazoan organisms such as rotifers, nematodes, copepods, tardigrades, and insect larvae can also be found. Edwards and others[18] describe cryoconite holes as "ice-cold hotspots". They also traced functional genes in cryoconite holes that are responsible for N, Fe, S, and P cycling. The mini lake ecosystems respire and photosynthesize at rates found in much warmer and more nutrient-rich habitats[11]. These findings emphasize the important role of microbial sequestration in supraglacial environments. Beside living communities in cryoconite holes, bare ice surfaces are inhabited by ice algae. Their physiology is well studied[19] but their spatial distribution has not been assessed[20]. Their presence in supraglacial environments decreases the albedo and hence promotes melting that leads to a nutrient outwash and nutrient input into downstream

habitats[9]. Increasing temperatures and hence, a higher availability of liquid water, affects the net ecosystem productivity in these icy ecosystems.

In supraglacial environments, photosynthetically active organisms transform inorganic carbon and nitrogen into organic, available sources for the microbial food web[21,22]. Until now there are few studies that estimate supraglacial carbon fluxes[11,20,23]. The discrepancy in proposed rates of carbon flux results from a low spatial and temporal data resolution. Further, the spatial distribution of supraglacial communities outside cryoconite holes is barely assessed. Cook and others[20] predicted in their models that supraglacial algal communities fix up to 11x more carbon than contemporary cryoconite holes due to their large surface coverage. The detection of supraglacial algal communities securing sample integrity is still impeded due to missing tools for in situ detection and quantification.

In response to difficulties in logistics, ice ecosystems are less frequently studied than habitats in temperate areas. Data resolution depends on the number of samples assessed and depend on the accessibility of the study sites. Standard sampling methods such as sawing, coring, and subsequent melting involve manipulation of the microbial community. For example, chlorophyll$_a$ (chl_a) assessment in solid ice samples is impossible with standard methods without substantial interference. Hence, melting-induced temperature changes within the investigated microbial communities are unavoidable. In response to the thermolability of the photosystem II and other cellular structures in psychrophiles[22], laboratory analyses of melted ice samples will always lead to a falsification of in situ conditions.

Non-destructive in situ measurements are the only reasonable way to obtain reliable data. This goal can be achieved using fluorescence-based methods. Due to their light harvesting function, chl_a and B-phycoerythrin (B-PE) are present in organisms that contribute to the carbon cycle in supraglacial environments, as has been proved by Anesio and others[11]. Hence, these fluorescent molecules are suitable biomarkers for the quantification of microbial mediated carbon fluxes in ice ecosystems.

In this study, we present the development, calibration, and applicability of a novel non-invasive tool for in situ quantification of chl_a and B-PE molecules in terrestrial and ice ecosystems. The prototype device is based on laser-induced fluorescent emission, also known as L.I.F.E. The optical instrument (**Figure 1**) captures fluorescent biomarker signatures after laser-induced fluorescence excitation. The procedure is nondestructive and can be performed at the study site or in a laboratory.

[Place **Figure 1** *here]*

The portable dual-wavelength kit weighs 4.5 kg and is used on a tripod in combination with an external computer. The field setup is quick and easy. The instrument is attached to the tripod, and the lens tube is attached to the device along with a USB cable and the camera cable. The external computer is connected to the instrument using a USB cable. The tripod legs are adjusted in such a way that the lens tube is directed towards and covers the specimen. Then, a 5 mW green laser hits the sample after passing a polarizing beam splitter that redirects polarized light towards the optical axis of the spectrometer. The specimen exhibits a fluorescent light, illustrated in red in **Figure 1**. Half of the collimated light passes the polarizing beam splitter and is focused through a servo-steered long-pass filter that removes the laser

signals. Next, the signal hits an aperture slit that consists of two adjustable razor blades. A prism spectrally separates the fine line of light orthogonal to the slit aperture before the signal is captured by the sensor. The procedure is repeated with a blue laser. The raw data are transferred automatically to a portable computer that is also used for the software operation.

The instrument is controlled by an external computer using a LabVIEW environment that synchronizes the picture-taking with the CCD camera, switching on/off lasers, and rotating the long-pass filter wheel. The graphical user interface (GUI) is divided into three main sections. The exposure adjustment is done manually. Although the correction between exposure time and signal intensity is linear (**Figure 2B**), the maximum exposure time is limited to 10 s because longer integration times lead to a significant decrease in the signal-to-noise-ratio. The comment field is used for the description of the sample (**Figure 2A**). In the right section, raw images are displayed as soon as the measurements are finished. This feature is crucial for immediate data evaluation in the field (**Figure 2C–E**). Red areas indicate overexposed pixels, which can be avoided by reducing the exposure time.

The subsequent raw data reduction process is decoupled from the image acquisition procedure and can be done at any time after image acquisition.

[Place **Figure 2** *and* **Figure 3** *here]*

The 12-bit gray-scale raw images show a spatial component due to the one-dimensional aperture slit and a spectral component due to the prism in front of the CCD (**Figure 3**). In response to optical constraints the raw images are distorted. Therefore, they need to be cropped and dewarped by applying a code that recognizes the degree of distortion. This is done with a software wizard (**Figure 4**). Next, the wavelength calibration is done with the 532 nm laser. The green light is produced by frequency doubling of a 1,064 nm infrared laser. Both wavelengths can be detected by the CCD and therefore, the spectral position of each pixel can be calculated in dewarped images automatically (**Figure 4**).

The picture is then cropped down to a given wavelength range (550–1,000 nm for green laser measurements and 400–1,000 for blue laser measurements). Gray values from each pixel in a selected pixel line are counted and summed up. A gray value can range from 0–255. After that, every pixel line accounts for one number. Further on-screen software instructions lead to the generation of a plot showing the gray value counts from each pixel line plotted against the spatial coordinates. This allows for a quantitative spatial discrimination of chl_a and B-PE simultaneously in the sample. Additionally, the spectral properties of a sample can be plotted from selected pixel lines automatically.

[Place **Figure 4** *here]*

PROTOCOL:

1. **Calibration and validation**

NOTE: For the pigment calibration, prepare dilution rows from stock solutions of chl_a and B-PE. The chl_a stock solution is diluted with acetone and B-PE is diluted with distilled sterile water. Later, 15 mL of each dilution step will be needed. Protect the pigments from light by

wrapping them with aluminum foil. Store the chl_a in a freezer and the B-PE in a refrigerator until further use. A detailed protocol for the dilution row follows in sections 1.1 for chl_a and 1.2 for B-PE. Both the chl_a and the B-PE laboratory calibration for pigment detection and quantification with the L.I.F.E. instrument is described below. A previous calibration[24] was made with the same pigments as in this study.

1.1. Chlorophyll$_a$ dilution row

1.1.1. Dissolve 1 mg of chl_a (purified from *A. nidulans* algae) with acetone in a 50 mL sample tube and dilute this chl_a stock solution with acetone to the following final concentrations: 1,000; 800; 640; 320; 160; 80; 40; 20; 10; 5; 1; and 0.5 ng/mL.

1.1.2. Transfer 15 mL of each dilution into 50 mL sample tubes and cover them in aluminum foil due to light sensitivity. Store the tubes in a -20 °C freezer until the calibration measurements are taken.

NOTE: The protocol can be interrupted here.

1.1.3. Measure the chl_a absorption features from each dilution in a double-beam spectrophotometer as triplicates and calculate the chl_a content as described by Lorenzen[25], which will be described in detail in section 2.2.2.

1.2. PE dilution row

1.2.1. Dilute a 4 mg/mL B-PE stock solution with sterile filtered water (pH = 7) to the following final concentrations: 1,000; 800; 640; 320; 160; 80; 40; 20; 10; and 5 ng/mL B-PE. Transfer 15 mL of each dilution in a 50 mL sample tube and cover it with aluminum foil. Store at 4 °C until further use.

NOTE: The protocol can be interrupted here.

1.3. Setup for calibration

1.3.1. Build a rack as shown in **Figure 5** to establish three measurement platforms, each 1.5 cm higher than the next.

NOTE: The rack and column height play an important role for the measurements because the surface of the liquids should remain in the focal point of the L.I.F.E. instrument as indicated in **Figure 5**.

1.3.2. Add 5 mL of the highest concentrated dilution in a polyscintillation plastic vial and put it on the highest point of the rack. Measure the fluorescence intensity.

1.3.3. Place the vial in the middle position of the rack and add another 5 mL (10 mL total volume). Measure the fluorescence intensity. Repeat the procedure at the lowest position on the rack with another 5 mL (15 mL total volume; total of 45 mm in column height).

NOTE: Adapt the exposure time for each dilution step to prevent detector saturation (gray values over 255 in 12-bit images) and for a sufficient signal-to-noise ratio of the weak fluorescence signals.

1.3.4 Repeat steps 1.3.2 and 1.3.3 with all dilutions (steps 1.1.1 and 1.2.1) of chl_a and B-PE.

1.3.5. Load the generated data files into the data reduction wizard to automatically count and sum up the gray values from each pixel line along the Y-axis (spatial distribution).

NOTE: Varying exposure times are compensated automatically by normalizing the fluorescence intensity to an integration time of 1 s.

1.3.6. Calculate the pigment area density with a Poisson regression analysis using the known concentrations from the dilution series and the normalized fluorescence intensities that were calculated. Then normalize the fluorescence counts from the three different column heights to 1.5 cm (5 mL) by multiplying the counts from each column height with a factor (factors 1, 0.5, and 0.33, for the 5 mL, 10 mL, and 15 mL concentration solutions, respectively).

[Place **Figure 5** *here]*

2. Sampling and sample processing

2.1. Collection of snow and ice

2.1.1. Collect snow and supraglacial ice from a glacier into sterile polyethylene bags and store them frozen until further processing.

NOTE: For this study, the samples were collected at Midtre Lovenbreen (MLB), a polythermal glacier near the research village Ny-Ålesund in the high Arctic Archipelago of Svalbard (78°53' N, 12°03' E).

2.1.2. Sample bacterial mats from the glacier forefield into sterile polyethylene bags and transport all samples to a laboratory for further processing.

2.1.3. Melt frozen material slowly in the dark at 4 °C. Filter liquid samples on GF/F filters (47 mm diameter) and note the filtered volume. Keep the filters frozen until further processing.

2.2. Chlorophyll$_a$ measurements

2.2.1. Using the L.I.F.E. instrument, measure the filter in four random areas, each in triplicates using the green and blue laser. Calculate the overall pigment concentration by multiplying the area density with the filtered area and filtered volume. Normalize the pigment concentration (µg/L) to a volume of 1 L.

2.2.2. Assess the chl_a contents of the GF/F filters with a laboratory standard according to the protocol by Lorenzen[25]. To do so, put each of the filters in a vial with 13 mL of acetone and store them in the dark at 4 °C overnight. Next, take a vial and place it on ice before sonication for 2 min at 50% power in continuous mode. Squeeze and remove the filter from the vial.

2.2.3. Attach tygon tubing to a syringe and remove the chl_a extraction-acetone mix from the vial. Replace the tygon tubing with a GF-5 filter holder. Transfer the solution into a quartz cuvette.

2.2.4. After calibrating the absorbance spectrometer for acetone, place the sample in the cuvette into the spectrometer and measure the absorbance features between 400–750 nm. Next, remove the cuvette from the spectrometer and add 200 µL of 2 M HCl to the sample. Then, repeat the absorbance measurement to measure the phaeophytin content in the sample.

2.3. Measurement of microbial activity via radiolabelled markers and impact of laser intensity and exposure time on productivity rates

CAUTION: Beware of the marker radioactivity (β-radiation). Use a laboratory coat, gloves, and goggles, and work under a fume hood in a licensed isotope lab.

2.3.1. For bacterial production transfer five aliquots of bacterial mats into sterile polyethylene bags. Inactivate the controls with formaldehyde to a 4% final concentration.

NOTE: Three aliquots are used for the ^{3}H-labeled leucine uptake and two aliquots are used as controls.

2.3.2. Expose the mats with a blue laser (405 nm, 5 mW) and with a green laser (532 nm, 5 mW) for 10 s and 30 s each. Repeat the procedure with 50 mW lasers. Then, inactivate the samples that were not treated with formaldehyde.

NOTE: One mat is used for only one laser exposure. Use non-exposed microbial mats as controls.

2.3.3. After the laser treatment, estimate the bacterial and primary production by incorporating ^{3}H-leucine and $NaH^{14}CO_3$, respectively. For bacterial production measurements, use five aliquots per sample (20 mL) and add formaline (4% final concentration) to two of the parallels, which serve as controls for the abiotic incorporation of the marker. Add ^{3}H-leucine (40 nM) to all samples of the various treatments and incubate them for 4 h under in situ conditions (0.1 °C). Terminate the reaction by adding formaline to the remaining live samples.

2.3.4. For bacterial production of bacterial mats, transfer labelled samples into cryovials. Extract cells with 5% trichloroacetic acid and centrifuge at 10,000 x *g* for 5 min according to the protocols by Kirchman[26] and Bell[27]. Add scintillation liquid and put the cryovial into a polyscintillation vial. Analyze the samples with a liquid scintillation counter and calculate the uptake rates.

NOTE: Three aliquots are used for the ^{3}H-labeled leucine uptake, two aliquots are used as controls.

2.3.5. For primary production, prepare five replicates of various treatments (100 mL), wrap two of them into aluminum foil to mimic the dark samples, and add $NaH^{14}CO_3$ (1 µCi) to all.

Incubate for 4 h in the ambient light and in situ temperature (0.1 °C). Terminate the reaction by darkening the remaining three replicates and filter the sample onto GF/F filters (25 mm diameter).

2.3.6. Add 100 µL of 2 N HCl to the filters to remove all excess carbon and let it air out under the fume hood. Dry the samples on a heating plate at 80 °C and place samples into polyscintillation vials.

2.3.7. To measure radioactive disintegrations per minute (dpm) of all treatments of primary and bacterial production, place the cryovials into polyscintillation vials and add 5 mL of scintillation cocktail. Measure dpm with a liquid scintillation counter and calculate the uptake rates.

REPRESENTATIVE RESULTS:

Laboratory calibration for B-PE

The response signals of the B-PE dilution row were measured with the L.I.F.E. instrument in a dark room at 20 °C (**Figure 6**). The count rate depended on both the concentration and the column height of the measured sample. Low concentration and low column height B-PE specimen fluoresced stronger compared to samples of the same concentration and higher column height.

[Place **Figure 6** *here]*

A Poisson regression was used for the final calibration line fit. There was a linear correlation between the area densities and pixel gray value counts. The function of the curve was y = 81.04x (**Figure 7**), which means that a gray value count rate of 8,104 in a 1 s exposed sample equaled an area density of 100 ng/cm^2 B-PE. The chl_a calibration is set up in an analogue manner. The function was y = 8.94x.

[Place **Figure 7** *here]*

Application on cryoconite samples from Svalbard and laboratory validation of data

The mean values of the L.I.F.E. measurements and the single measurements of the same samples derived from conventional extraction using acetone and subsequent analysis with a spectrophotometer are illustrated in **Figure 8**.

[Place **Figure 8** *here]*

Chl_a contents ranging from 48 µg/L–67 µg/L were underestimated, and lower chl_a contents ranging from 0.7 µg/L–7 µg/L were overestimated by the L.I.F.E. prototype. The standard deviations from the L.I.F.E. measurements were low.

Comparison of spectral data from in situ measurements with laboratory standards

Chl_a spectra were comparable between cryoconite samples and those from purified from *A. nidulans* algae. The fluorescence peaks in all samples were located at 700 nm–710 nm. However, spectra derived from cryoconite samples showed higher noise signals between 400 nm–650 nm and from 800 nm–1,000 nm compared to spectra of the chl_a pigment standard (**Figure 9**).

[Place **Figure 9** *here]*

Automated cryoconite grain analysis

In an example of an automated analysis of a cryoconite hole (**Figure 10**), the highest pigment area densities were observed at pixel line 50. The sample spectrum after excitation with a 532 nm laser showed a peak with a cut off at a gray value of 255 in response to oversaturation of the sensor. This peak derived from the green laser and not from the fluorescent signal.

[Place **Figure 10** *here]*

Impact of laser excitation on productivity in bacterial mats

Neither primary nor bacterial productivity were affected when increasing the power of the laser and/or the exposure time (**Figure 11**). No significant differences were detected under laser treatments with increased power.

[Place **Figure 11** *here]*

FIGURE LEGENDS:

Figure 1: The L.I.F.E. prototype. Left: Photo of the instrument without a protective lid. **Right:** Schematic illustration of the instrument. Total mass = 5.4 kg (laser and optics = 4.025 kg, laptop = 1.37 kg). Aluminum frame = 32.5 cm x 20.3 cm x 6.5 cm. Optical tube: 18.4 cm x 4 cm (diameter). CCD: bluefox mv220g sensor; F: servo-steered long-pass filters (450 nm and 550 nm); L: optical lenses; M1: mirrors; M2: dichroic mirror; MC: microcontroller; P: prism; PBS: polarizing beam splitter; S: slit aperture made of adjustable razor blades. Scale bar = 70 mm.

Figure 2: L.I.F.E. graphical user interface for the data acquisition and raw data evaluation. (**A**) The software enables manual text input for sample descriptions. (**B**) The exposure time can be adjusted before the measurement. (**C–E**) The raw images are displayed on the right side of the interface. (**E**) Red colors indicate a saturation of the sensor. (**F**) The activation of the **RUN MEASUREMENT** button triggers the data acquisition process. In the array (**G**), all commands executed automatically during data acquisition are displayed.

Figure 3: Example of a raw image. Left: Raw data of chl_a standard in acetone solution, recorded with the L.I.F.E instrument. Due to the optical properties of the device, the signal is displayed as a warped line. **Right:** Interpretation of the raw image per pixel (px). The spectral axis (5 nm/px resolution) is plotted against the spatial axis (30 µm/px resolution).

Figure 4: Dewarping raw images. Left: Raw image captured with a green laser. No filter was used. Signals are displayed at 532 nm and 1,064 nm. Exposure time = 0.015 s. **Center:** The cropped 532 nm signal is used as a reference line to dewarp a set of images. **Right:** The dewarped image from the raw image source.

Figure 5: Setup for the L.I.F.E. calibration with chl_a and B-PE under laboratory conditions. (**A**) Lens tube of the instrument. (**B**) Green laser for B-PE excitation. (**C**) Blue laser for chl_a excitation. (**D**) Scintillation vial. (**E**) Focal point of the L.I.F.E. instrument. (**F**) B-PE/water or chl_a/acetone solution with 5 mL, 10 mL, and 15 mL. (**G**) Spacers that keep the surface of each solution at the focal plane for three different volumes.

Figure 6: B-PE laboratory calibration. B-PE content and column density calibration is shown. Normalized count rates were calculated for a column height of 1.5 cm. Reprint with permission[28].

Figure 7: Final calibration curve for B-PE. The gray value counts were normalized to an exposure time of 1 s and plotted against the area density. Reprint with permission[28].

Figure 8: Data validation with natural samples. The samples (MLB) are ranked by chl_a content, based on the results of a laboratory spectrophotometer (single values) and compared with the chl_a fluorescence data measured on four random areas per filter. The error bars represent the standard deviation of the L.I.F.E. measurements.

Figure 9: Spectral data interpretation. Measurements of four cryoconite granules (blue) and a chl_a standard pigment solution (red) after excitation with 405 nm lasers. The spectra were recorded 1 year after sample collection. The samples were kept frozen and were not exposed to light prior to the measurement. In response to wavelength calibration issues, the fluorescence peak is located at 700 nm–710 nm instead of 680 nm.

Figure 10: Automated data analysis of a single cryoconite granule with a diameter of 1 mm. The sample was collected at Vestre Brøggerbreen (VBB) and measured within 4 h after sampling in a dark laboratory room at the Arctic Station (GB) facility in Ny-Ålesund. The left column shows B-PE measurements and the right column represents chl_a data. The raw images are displayed on top. Laser-induced fluorescence responses are displayed in gray. Red areas indicate the response from standard pigments. The middle section illustrates the spatial distribution of the target pigments. The spectral properties of the fluorescence signal are displayed in the lower images.

Figure 11: Productivity measurements of samples from Svalbard. Bacterial mats were exposed with green and blue lasers of varying laser intensities and exposure times. The data are colored according to the laser wavelength source (green and blue).

Figure 12: Fluorescence signals from thick (A) and thin (B) filter cakes on a GF/F filter. (**A**) Self-shading prevents laser-induced fluorescence from deeper layers, which results in an underestimate of the actual pigment concentration. (**B**) Fluorescence emission from filter cake with overlay by filter reflections. (**C**) Raw data show filter reflection (gray). The spectral property of a laboratory derived chl_a fluorescence pattern is illustrated in red. Scale bar = 45 mm.

Figure 13: Mineral fluorescence from a geode rock, found in Ny-Ålesund. The rock was excited with a 532 nm 50 mW laser (**A**) and a 405 nm 50 mW laser (**B**). Both pictures were captured with a polarization filter attached on the lens, which led to a falsification of the actual fluorescence colors. (**C**) True color image without the use of a polarization filter under daylight conditions. Scale bar = 40 mm.

Figure 14: Cryoconite hole with liquid water on top. (**A**) Cryoconite on glacier with L.I.F.E. lens tube. Scale bar = 70 mm. (**B**) The sediment layer (red) is very thin. Stray light bleeds through

the cryoconite layer. (**C**) The sediment layer is thick enough to block the stray light from beneath. This type of cryoconite hole is measurable with the L.I.F.E. instrument.

DISCUSSION:

Calibration

There was a linear correlation between pigment concentration and fluorescence intensity after normalizing photon counts to an exposure time of 1 s. Samples with low column height and low pigment concentrations led to an overestimation of the target pigments, compared to higher column heights with the same pigment concentration. Further, weak fluorescence signals required long exposure times for sufficient photon counts on the sensor. However, long integration times also increased the amount of stray light on the sensor, resulting in a decrease of the signal-to-noise ratio. In its current version, the software cannot distinguish between noise and signal during the data reduction process. Hence, low fluorescence intensity measurements led to a pigment overestimation because noise was counted as a signal that derived from the target pigments. Further, fluorescence intensities from more concentrated pigment solutions showed a greater variability than low concentration solutions. This effect could be explained by absorption processes within the pigment solutions that were used for the calibration curve.

Data validation for chlorophyll$_a$ quantification

After filtering ice and snow samples, the three-dimensional samples almost appeared as a two-dimensional specimen on the filter. This justified a direct comparison between L.I.F.E (area density) and spectrophotometric data (volumetric measurement).

The data set (**Figure 8**) indicated that high pigment concentration leads to an underestimation, whereas low pigment concentration leads to an overestimation of the actual value. This effect can be explained by the thickness of the filter cake and hence, the volumetric character of the sample. The laser penetration depth depended on the optical density and thickness of the specimen. High pigment contents were underestimated because the laser could not induce pigment fluorescence in deeper layers. However, in thin filter cakes, low fluorescence signals were captured due to low area densities of pigments. Apparently, the filter itself showed laser-induced signals after passing the 450 nm long-pass filter (**Figure 12**). This signal was misleadingly counted as fluorescence signal derived from chl$_a$. Thus, thin and too thick filter cakes are difficult to measure with the L.I.F.E. instrument.

[Place **Figure 12** *here]*

Limitations of the L.I.F.E. prototype

During data reduction, the MATLAB coded software interpreted the raw images by summing up pixel lines within a given wavelength range. The current version of the software did not distinguish between organic and inorganic derived signals. The presence of multiple signals might lead to an overestimation of the actual pigment content. Long exposure times due to low fluorescence intensities led to a decrease of the signal-to-noise ratio, promoting the effect as described above (see **Figure 8** and **Figure 12**).

A geode rock shown in **Figure 13** exhibited red fluorescent light when exposed with green and blue light. Currently, it is not clear whether the fluorescence resulted from minerals or from porphyrin-based molecules. Hence, an overlay of biological and nonbiological signals may limit

the application of this method and require the establishment of a fluorescence database specifically made for the L.I.F.E. prototype.

[Place **Figure 13** *here]*

Beutler and others[29] concluded that characteristic emission spectra of cyanobacteria in marine ecosystems depend on environmental conditions. Also, the metabolic state has an impact on the fluorescence properties in phototrophic organisms[30]. The L.I.F.E instrument may distinguish between the algal and cyanobacterial fluorescence pattern by using bio-fingerprint libraries that contain spectral information of the specimen correlated with environmental conditions.

In dark-adapted chl_a molecules, all reaction centers are fully oxidized and available for photochemistry and no fluorescence yield is quenched[31]. Using the L.I.F.E. procedure, a specimen is first excited by a 532 nm laser (green) and then with a 405 nm laser (blue). During the second excitation by the blue laser, chl_a might show a decreased fluorescence response due to prior excitation by the green laser. Chl_a absorbs energy at 532 nm wavelength, despite its distance from its absorption maximum wavelength[32]. Before the actual chl_a measurement at 405 nm, the green laser may cause photochemical reactions, activating quenching mechanisms in the target pigments. Further, pre-illumination of marine phototrophic organisms did not lead to a change in spectral norm curves between 450 nm–600 nm while the standard deviation in fluorescence intensities increased by 25%[29]. Depending on the species, fluorescence intensities even increased in response to prior excitation. This topic requires further investigation.

Applicability

We tested the L.I.F.E. instrument in various habitats with an emphasis on cryoconite holes. The laser was successfully applied in soil and biofilm habitats because of the absence of ambient light during the measurement. Cryoconite granules could be measured when sediment layers blocked light from beneath the hole (**Figure 14 A**,**C**). Thin sediment cryoconite holes were permeable for stray light from beneath (**Figure 14B**). Stray light interferes with the measurement. Thus, pigment concentration in bare ice surfaces is not measurable under daylight conditions yet. Signal processing efforts are currently underway to enable operation of the system in high ambient light conditions.

[Place **Figure 14** *here]*

In conclusion, our L.I.F.E. instrument detected photoautotrophic organisms in terrestrial habitats such as soils, bacterial mats, biofilms, and in cryoconite holes on glacial surfaces. The target molecules were chl_a and B-PE. The spatial resolution was 30 µm/px. The detection limit for chl_a was 250 pg/mL and 2 ng/mL for B-PE. After a laboratory calibration we were able to quantify pigment content in samples that were collected at our study site in the Arctic. We applied self-programmed software for an automated data reduction process. The effects of the presence of minerals and changing light conditions during the measurements require further investigation.

With climate warming, increasing temperatures lead to enhanced availability of liquid water, which results in higher biological activity on icy surfaces of autotrophic and heterotrophic

nature. Vigorous efforts should be made to detect heterotrophic organisms in situ to give a full picture of active life in the cryosphere. This could be tested with other target pigments and appropriate laser excitation wavelengths. Hence, L.I.F.E. provides a suitable monitoring system providing high temporal and spatial resolution for supraglacial conditions in context with global change as well as possible astrobiological applications.

ACKNOWLEDGEMENTS:

The authors gratefully thank Colonel (IL) J.N. Pritzker, the Tawani Foundation, USA, the Austrian Federal Ministry of Science, Research and Economy (Sparkling Science SPA04_149 and SPA05_201), Alpine Forschungsstelle Obergurgl (AFO), Austrian Space Forum (ÖWF), Roman Erler from the Hintertuxer Natur Eis Palast, the Austrian Federal Forestry and Base Manager Nick Cox from the Arctic Station in Ny Alesund (Svalbard). We are also indebted to Sabrina Obwegeser, Carina Rofner, and Fabian Drewes for their help during filming. Finally, we want to thank James Bradley for giving the voice for the concomitant video.

DISCLOSURES:

The authors have nothing to disclose.

REFERENCES:

1. Boyd, E. S., Skidmore, M., Mitchell, A. C., Bakermans, C., Peters, J. W. Methanogenesis in subglacial sediments. *Environmental Microbiology Reports*. **2**, 685–692 (2010).
2. Sattler, B., Puxbaum, H., Psenner, R. Bacterial growth in supercooled cloud droplets. *Geophysical Research Letters*. **28**, 239–242 (2001).
3 Good, P. et al. A review of recent developments in climate change science. Part I: Understanding of future change in the large-scale climate system. *Progress in Physical Geography*. **35**, 281–296 (2011).
4. Fountain, A. G. et al. The Disappearing Cryosphere: Impacts and Ecosystem Responses to Rapid Cryosphere Loss. *BioScience*. **62**, 405–415 (2012).
5. Rignot, E., Mouginot, J., Morlighem, M., Seroussi, H., Scheuchl, B. Widespread, rapid grounding line retreat of Pine Island, Thwaites, Smith, and Kohler glaciers, West Antarctica, from 1992 to 2011. *Geophysical Research Letters*. **41**, 3502–3509 (2014).
6. McMillan, M. et al. Increased ice losses from Antarctica detected by CryoSat-2. Geophys. Res. Letters. *Geophysical Research Letters*. **41**, 3899–3905 (2014).
7. Barletta, V. R. et al. Glacier shrinkage and modeled uplift of the Alps. *Geophysical Research Letters*. **33**, L14307 (2006).
8. Nuth, C. et al. Decadal changes from a multi-temporal glacier inventory of Svalbard. *The Cryosphere*. **7**, 1603–1621 (2013).
9. Takeuchi, N., Kohshima, S., Seko, K. Structure, formation, and darkening process of albedo-reducing material (cryoconite) on a Himalayan glacier: A granular algal mat growing on the glacier. *Arctic Antarctic and Alpine Research*. **33**, 115–122 (2001).
10. Takeuchi, N. Optical characteristics of cryoconite (surface dust) on glaciers: the relationship between light absorbency and the property of organic matter contained in the cryoconite. *Annals of Glaciology*. **34**, 409–414 (2002).
11. Anesio, A. M., Hodson, A. J., Fritz, A., Psenner, R., Sattler, B. High microbial activity on glaciers: importance to the global carbon cycle. *Global Change Biology.* **15**, 955–960 (2009).
12. Anesio, A. M. et al. Carbon fluxes through bacterial communities on glacier surfaces. *Annals of Glaciology*. **51**, 32–40 (2010).
13. Storrie-Lombardi, M. C., Sattler, B. Laser-Induced Fluorescence Emission (L.I.F.E.): In Situ

623 Nondestructive Detection of Microbial Life in the Ice Covers of Antarctic Lakes. *Astrobiology*.
624 **9**, 659–672 (2009).
625 14. Murray, A. E. et al. Microbial life at −13 °C in the brine of an ice-sealed Antarctic lake.
626 *Proceedings of the National Academy of Sciences of the United States of America*. **109**, 20626–
627 20631 (2012).
628 15. Edwards, A. et al. A distinctive fungal community inhabiting cryoconite holes on glaciers in
629 Svalbard. *Fungal Ecology*. **6**, 168–176 (2013).
630 16. Miteva, V. Bacteria in Snow and Glacier Ice. In *Psychrophiles: from Biodiversity to*
631 *Biotechnology*. Edited by Margesin, R., Schinner, F., Marx, J.-C., Gerday, C., 31–50, Springer
632 Berlin Heidelberg. Berlin/Heidelberg, Germany (2008).
633 17. Yallop, M. L. et al. Photophysiology and albedo-changing potential of the ice algal
634 community on the surface of the Greenland ice sheet. *The ISME Journal*. **6**, 2302–2313 (2012).
635 18. Edwards, A. et al. A metagenomic snapshot of taxonomic and functional diversity in an
636 alpine glacier cryoconite ecosystem. *Environmental Research Letters*. **8**, 035003 (2013).
637 19. Remias, D. et al. Characterization of an UV-and VIS-absorbing, purpurogallin-derived
638 secondary pigment new to algae and highly abundant in Mesotaenium berggrenii
639 (Zygnematophyceae, Chlorophyta), an extremophyte living on glaciers. *FEMS Microbiology*
640 *Ecology*. **79**, 638–648 (2012).
641 20. Cook, J. et al. An improved estimate of microbially mediated carbon fluxes from the
642 Greenland ice sheet. *Journal of Glaciology*. **58**, 1098–1108 (2012).
643 21. Mueller, D. R., Vincent, W. F., Pollard, W. H., Fritsen, C. H. Glacial cryoconite ecosystems:
644 a bipolar comparison of algal communities and habitats. *Nova Hedwigia Beiheft*. **123**, 173–198
645 (2001).
646 22. Morgan-Kiss, R. M., Priscu, J. C., Pocock, T., Gudynaite-Savitch, L., Huner, N. P. A.
647 Adaptation and Acclimation of Photosynthetic Microorganisms to Permanently Cold
648 Environments. *Microbiology and Molecular Biology Reviews*. **70**, 222–252 (2006).
649 23. Hodson, A. et al. The cryoconite ecosystem on the Greenland ice sheet. *Annals of*
650 *Glaciology*. **51**, 123–129 (2010).
651 24. Tilg, M. et al. L.I.F.E.: laser induced fluorescence emission, a non-invasive tool to detect
652 photosynthetic pigments in glacial ecosystems, *Proceedings SPIE*. **8152**, Instruments,
653 Methods, and Missions for Astrobiology XIV, 81520I (2011).
654 25 Lorenzen, C. J. Determination of chlorophyll and pheo-pigments: spectrophotometric
655 equations. *Limnology & Oceanography*. **12**, 343–346 (1967).
656 26. Kirchman, D. Measuring bacterial biomass production and growth rates from leucine
657 incorporation in natural aquatic environments. *Methods in Microbiology*. 227–238 (2001).
658 27. Bell, R. T. Estimating production of heterotrophic bacterioplankton via incorporation of
659 tritiated thymidine. In *Handbook of methods in aquatic microbial ecology*. Edited by Kemp, P.
660 F., Cole, J. J., Sherr, B. F., Sherr, E. B., 495–503, CRC press. Boca Raton, FL (1993).
661 28. Groemer, G. et al. Field trial of a dual-wavelength fluorescent emission (L.I.F.E.) instrument
662 and the Magma White rover during the MARS2013 Mars analog mission. *Astrobiology*. **14**,
663 391–405 (2014).
664 29. Beutler, M. *Spectral fluorescence of chlorophyll and phycobilins as an* in situ *tool of*
665 *phytoplankton analysis-models, algorithms and instruments*. Doctoral dissertation. Christian-
666 Albrechts Universität Kiel (2003).
667 30. Govindjee, Krogmann, D. Discoveries in Oxygenic Photosynthesis (1727–2003): A
668 Perspective. *Photosynthesis Research*. **80**, 15–57 (2004).
669 31. Corrêa, D. S. et al. Reverse saturable absorption in chlorophyll A solutions. *Journal of*
670 *Applied Physics B*. **74**, 559–561 (2002).

671 32. Kaňa, R. et al. The slow S to M fluorescence rise in cyanobacteria is due to a state 2 to state
672 1 transition. *Biochimica et Biophysica Acta*. **1817**, 1237–1247 (2012).

Figure 1

Click here to access/download;Figure;Figure 1_R2.pdf

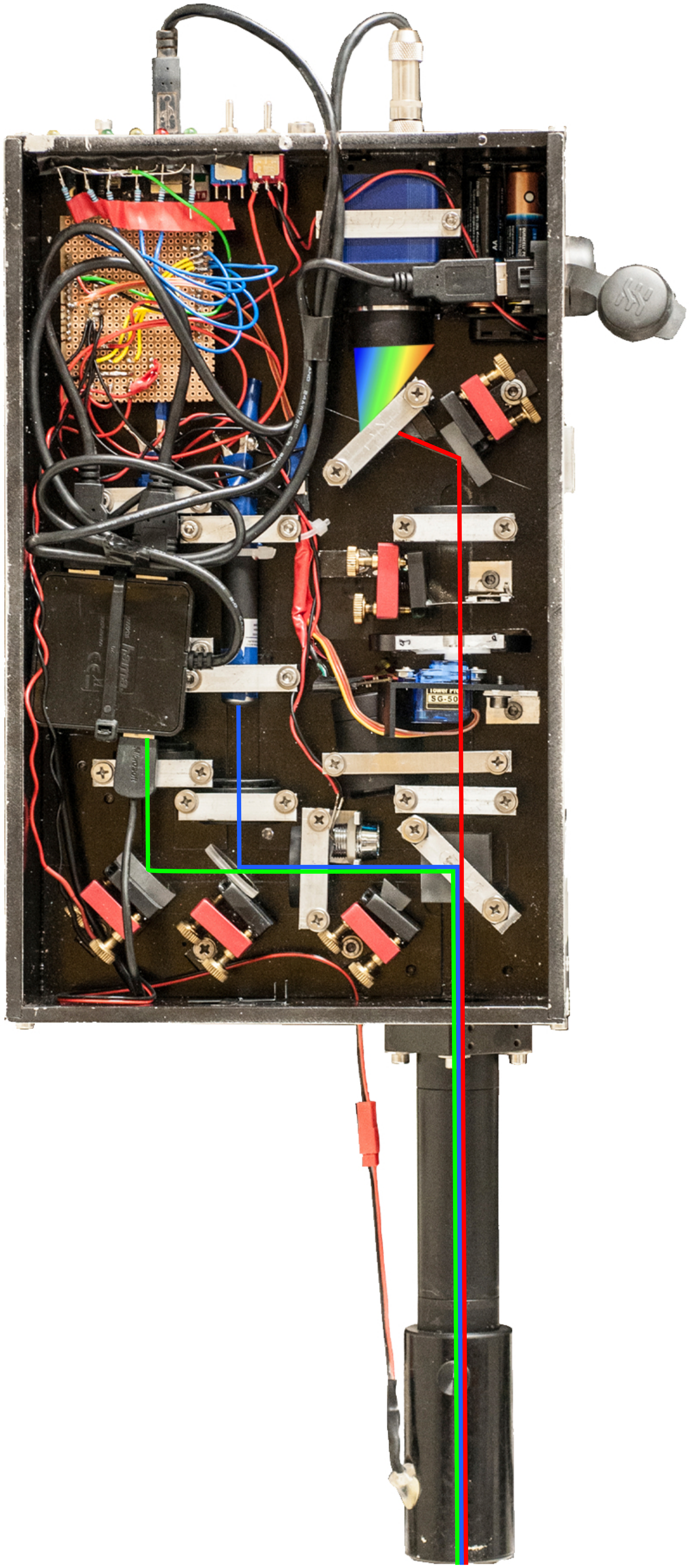

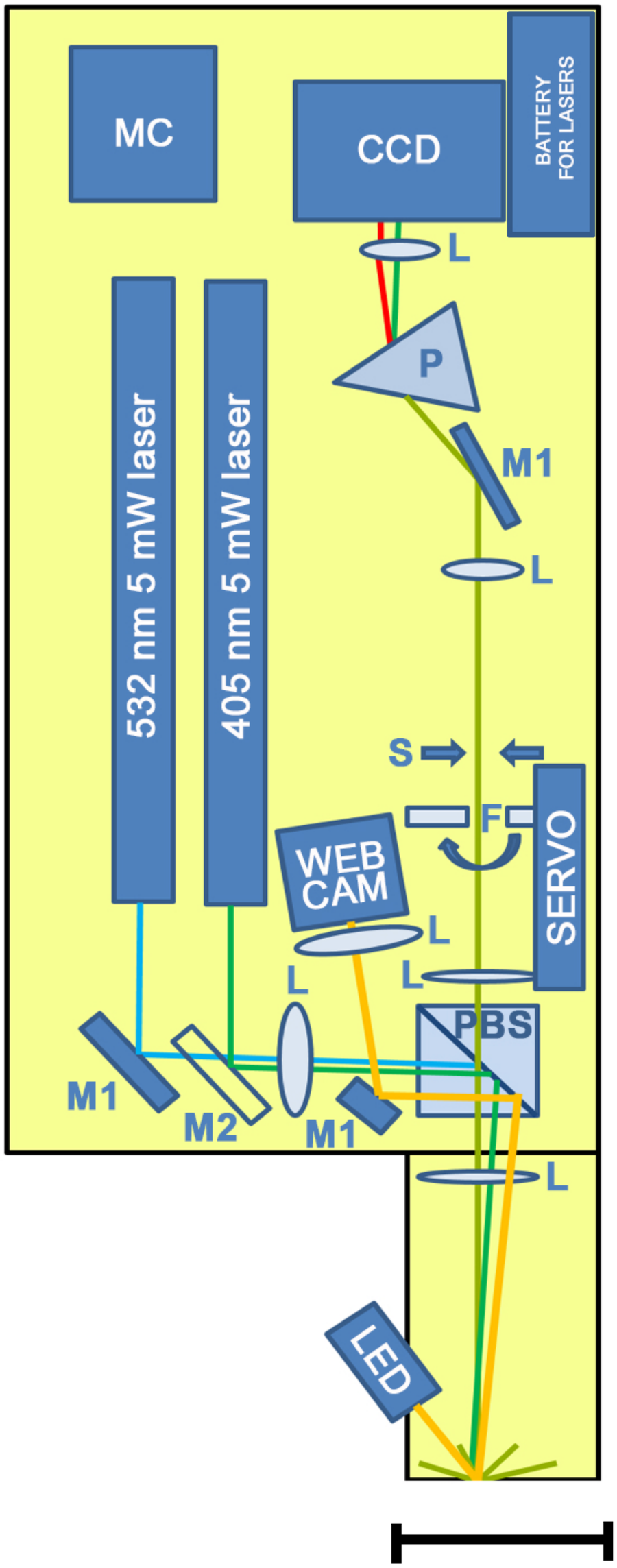

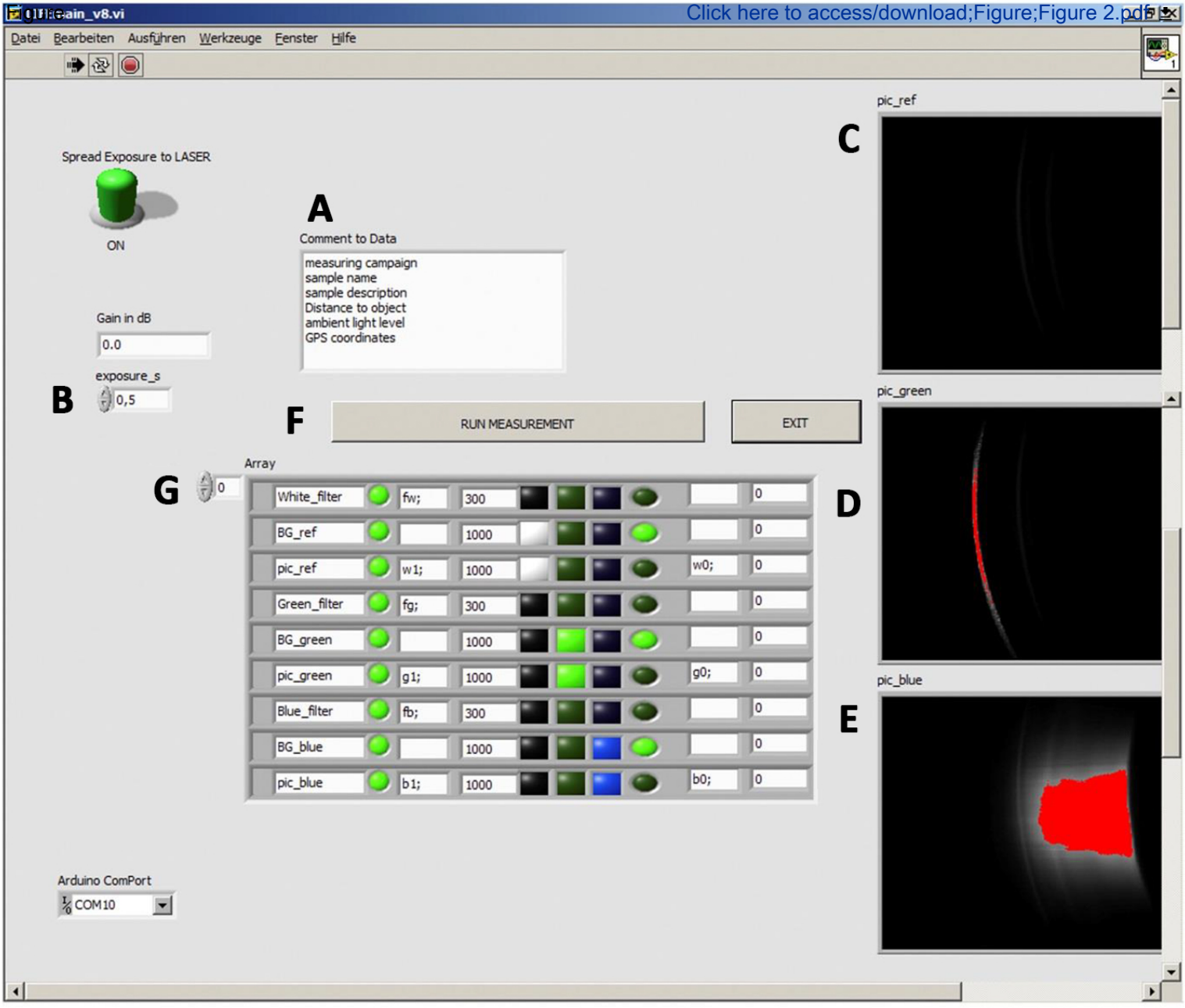

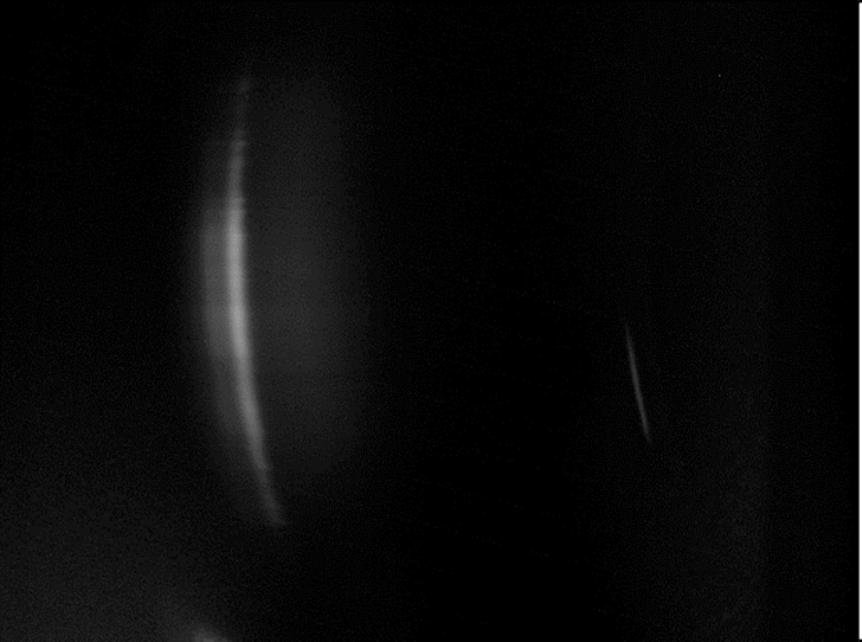

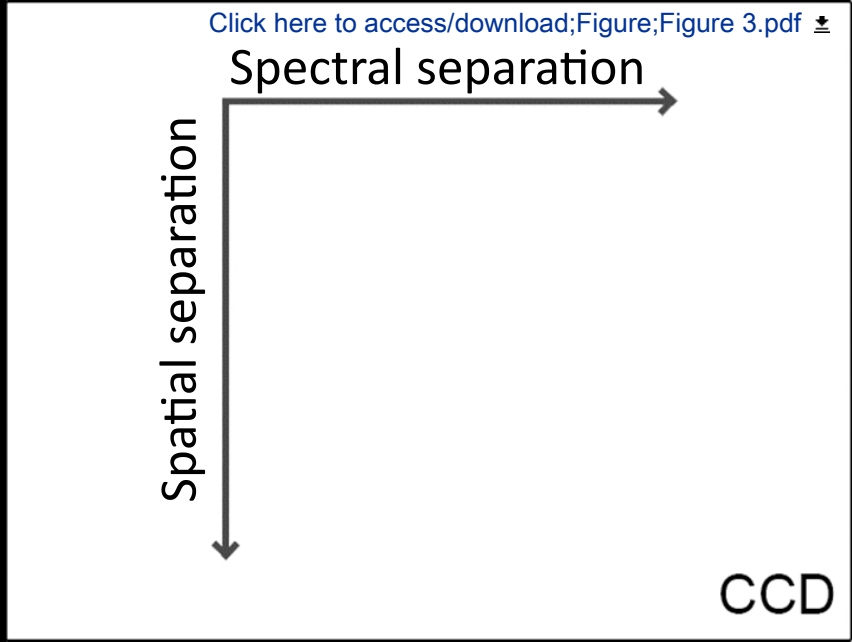

Figure

Click here to access/download;Figure;Figure 4.pdf

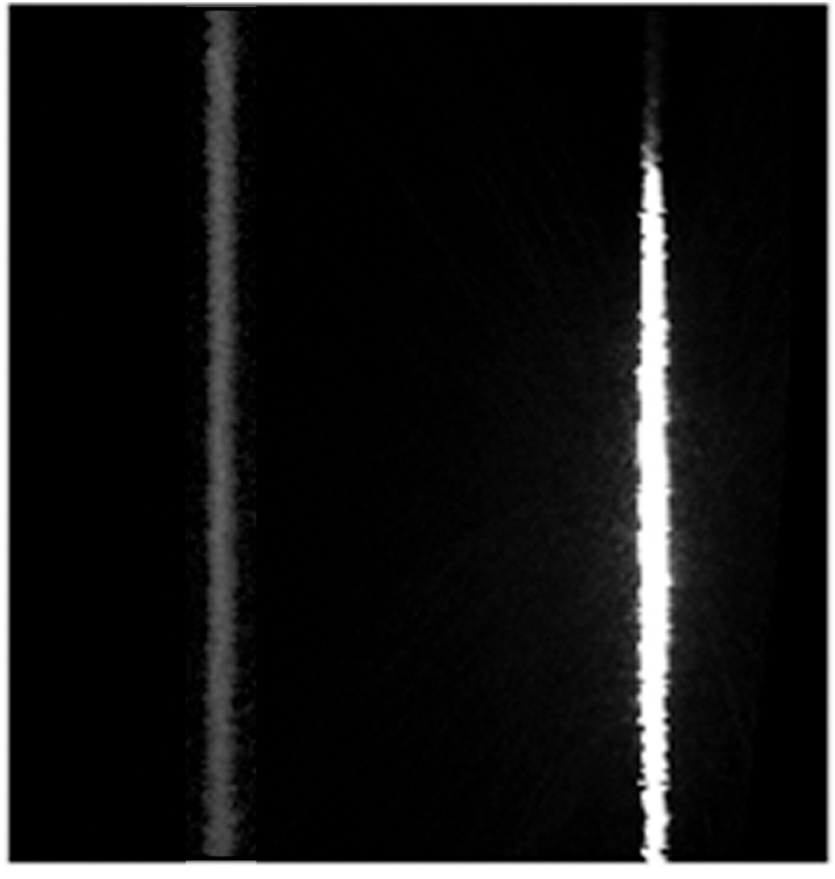

Figure

Click here to access/download;Figure;Figure

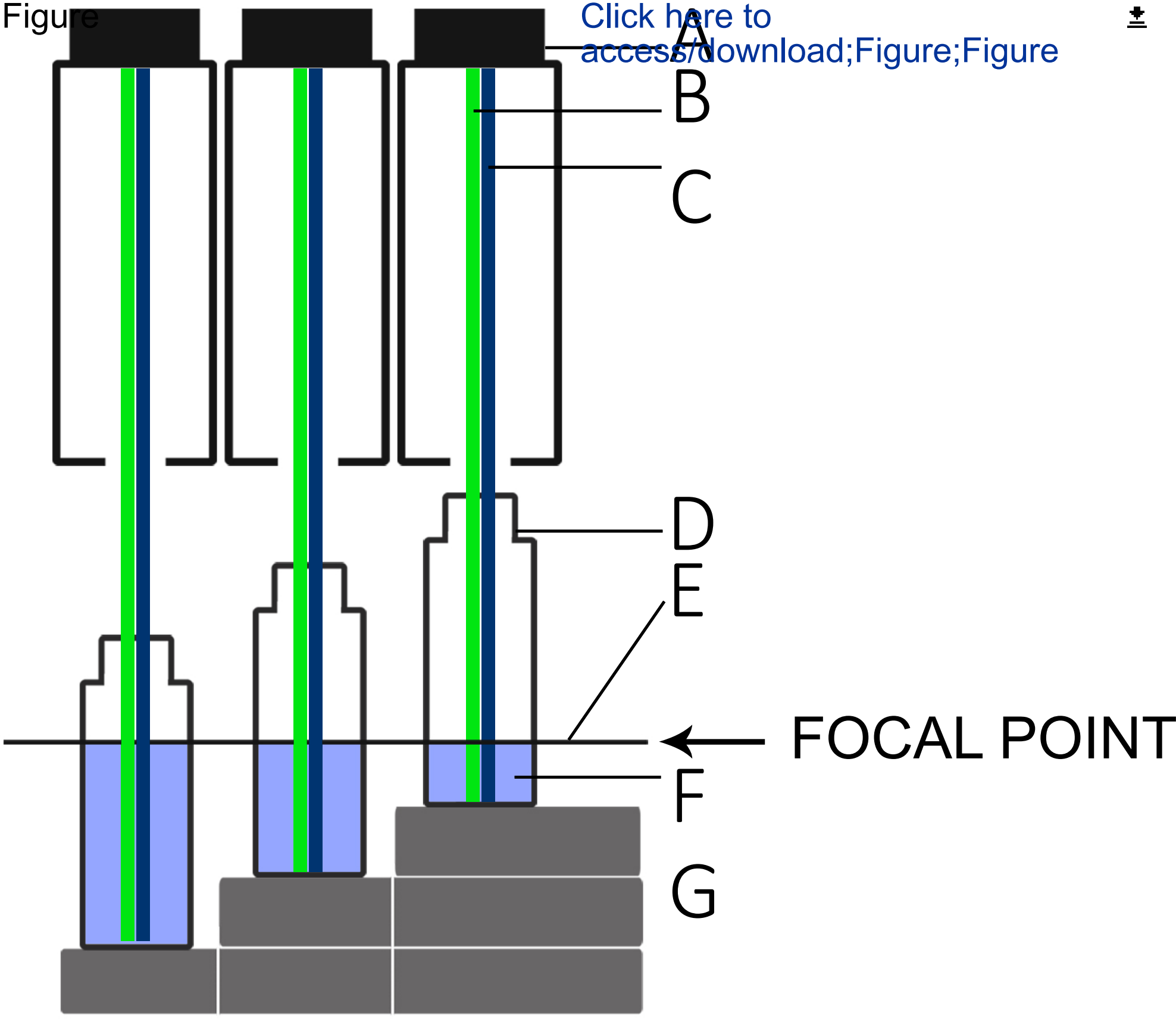

Figure

Click here to access/download;Figure;Figure 6.pdf

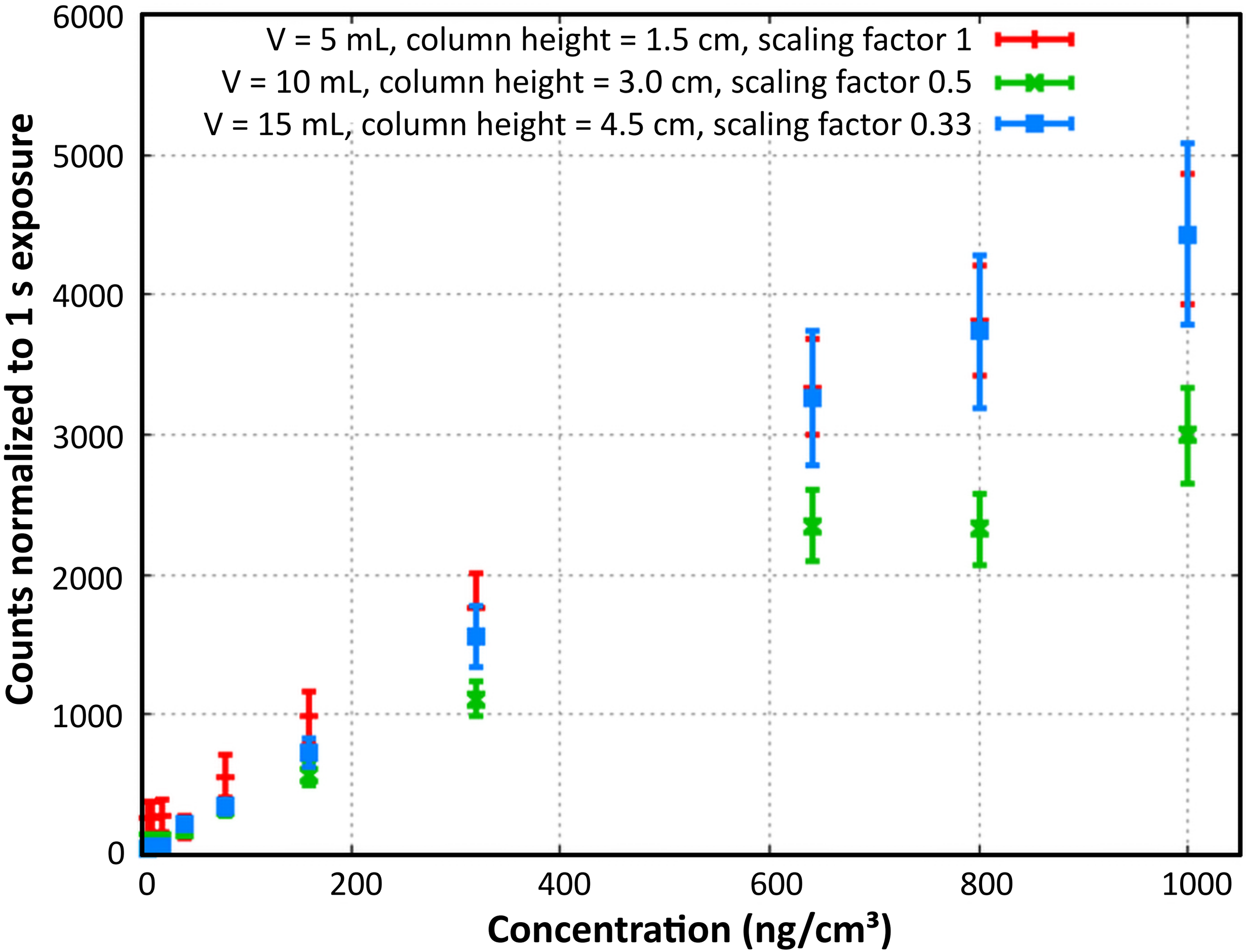

Figure

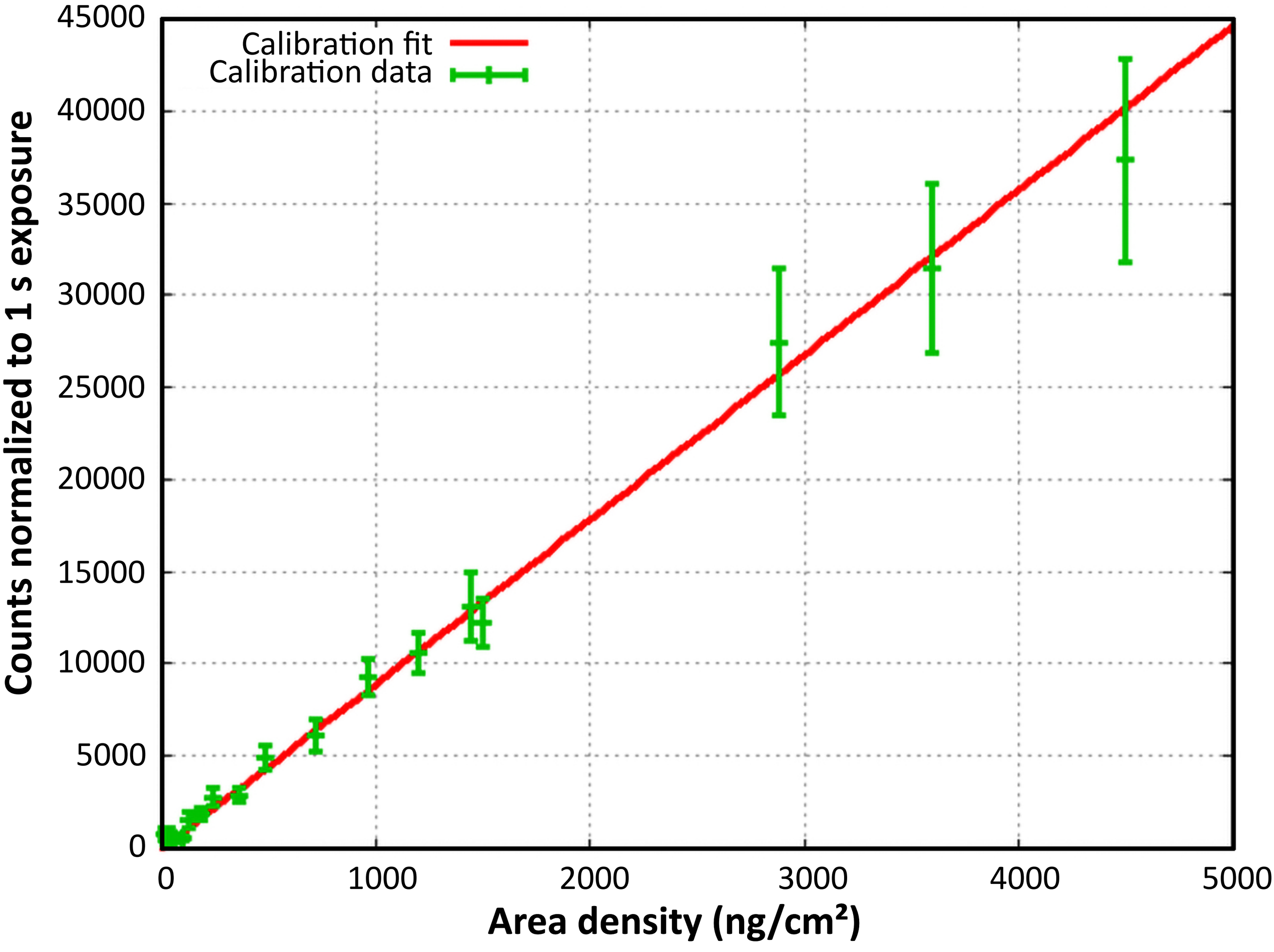

Figure

Click here to access/download;Figure;Figure 8.pdf

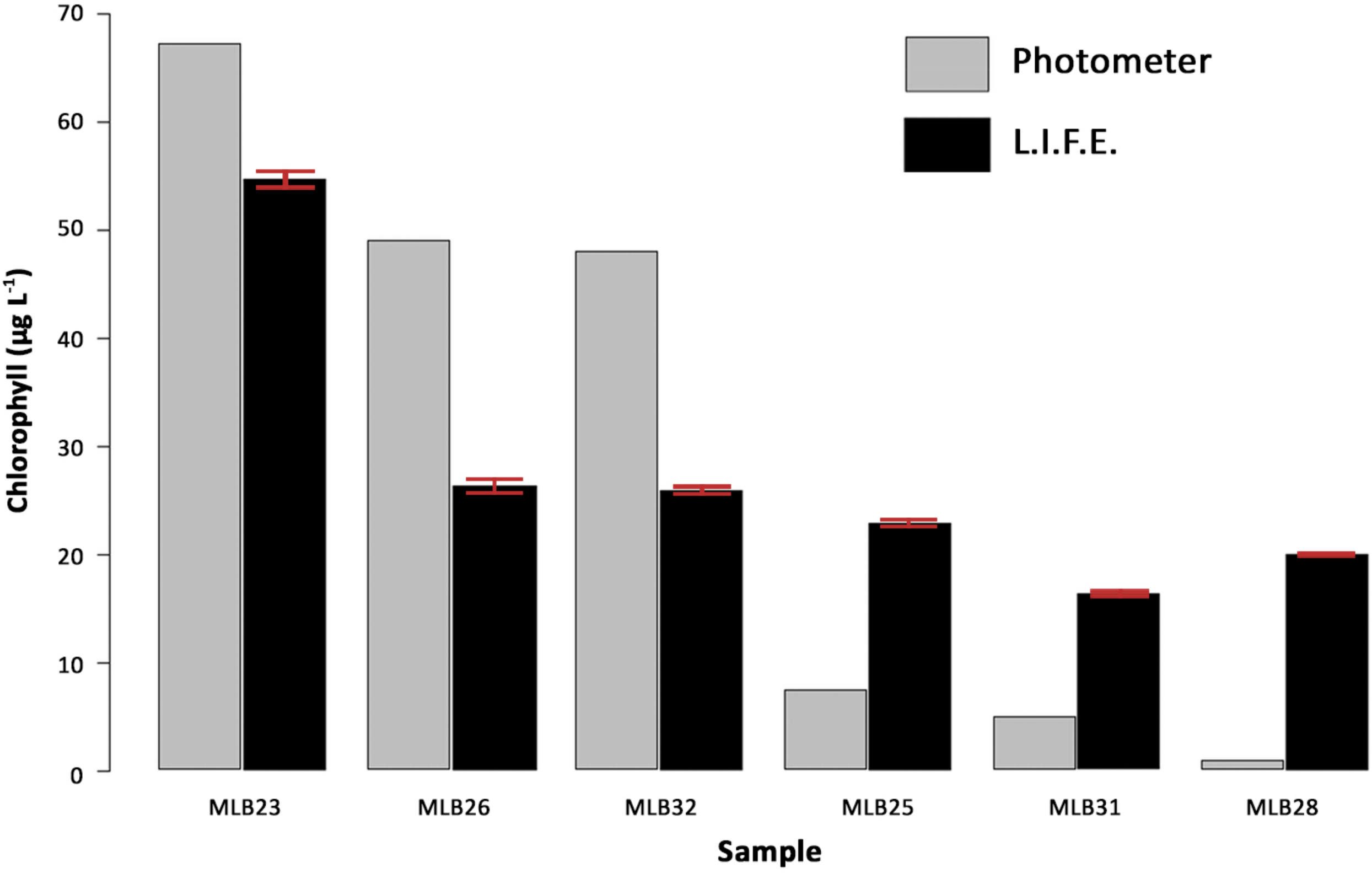

Figure

Click here to access/download;Figure;Figure 9.pdf

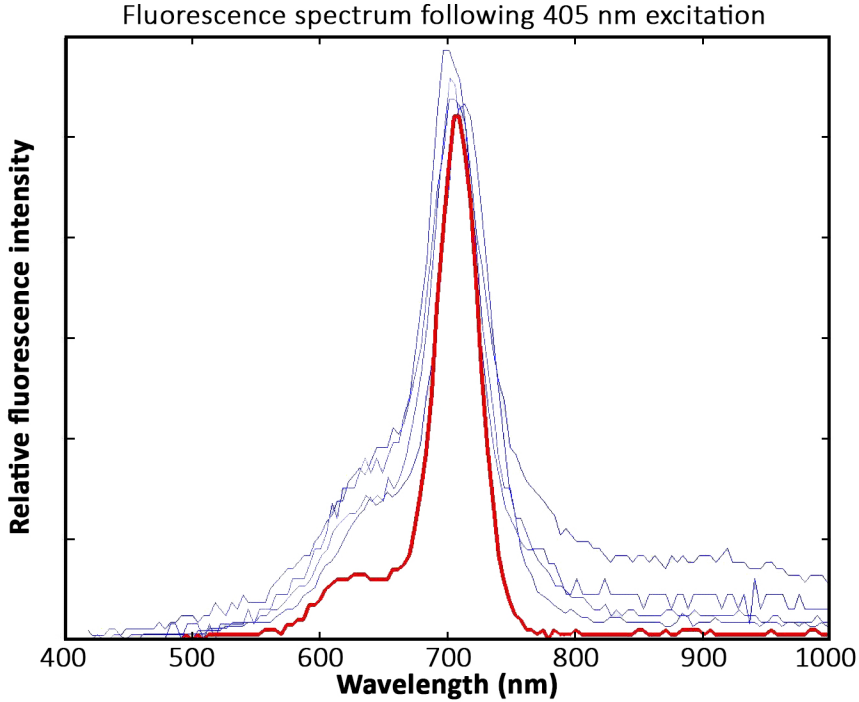

Figure

Click here to access/download;Figure;Figure 10.pdf

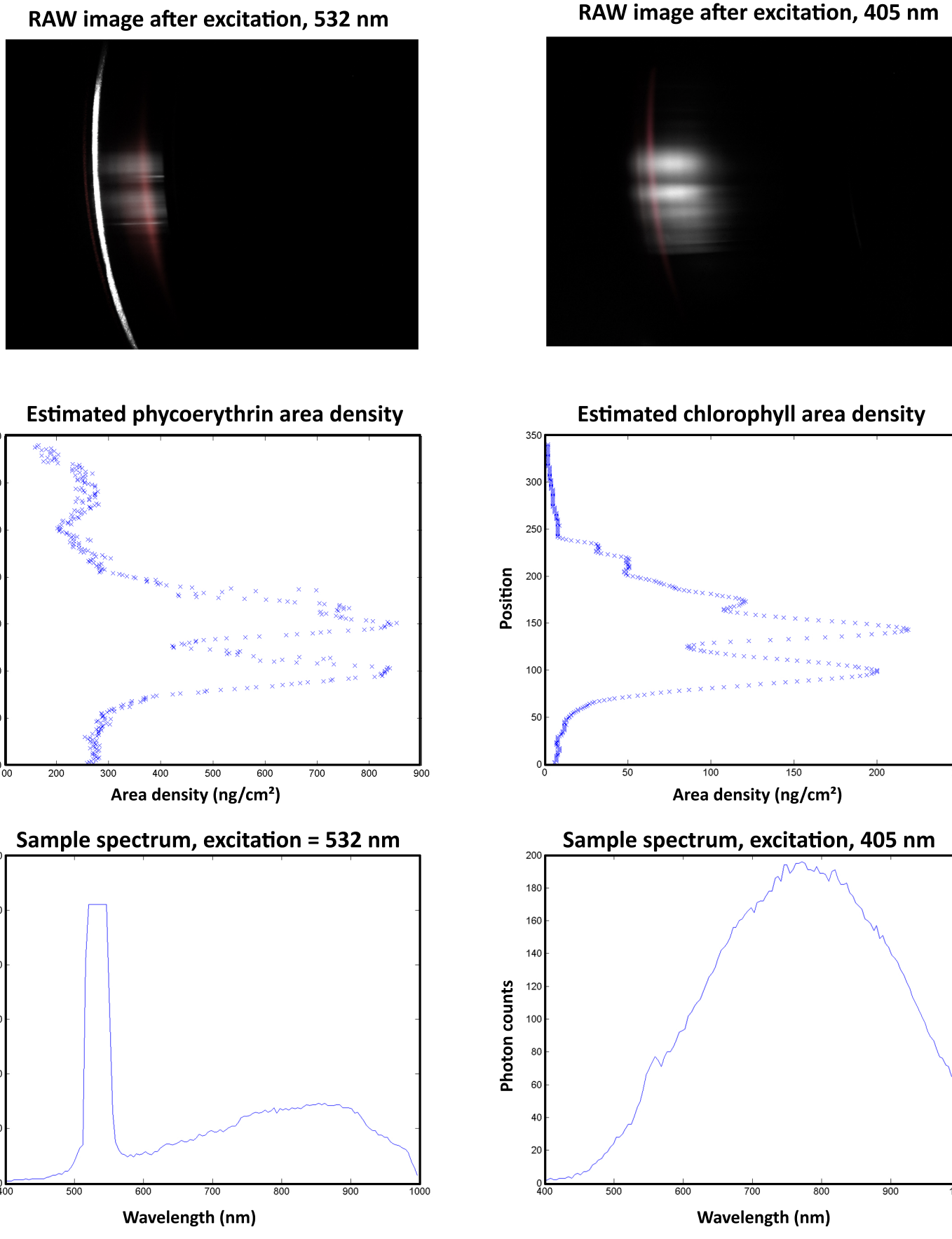

Figure

Click here to access/download;Figure;Figure 11.pdf

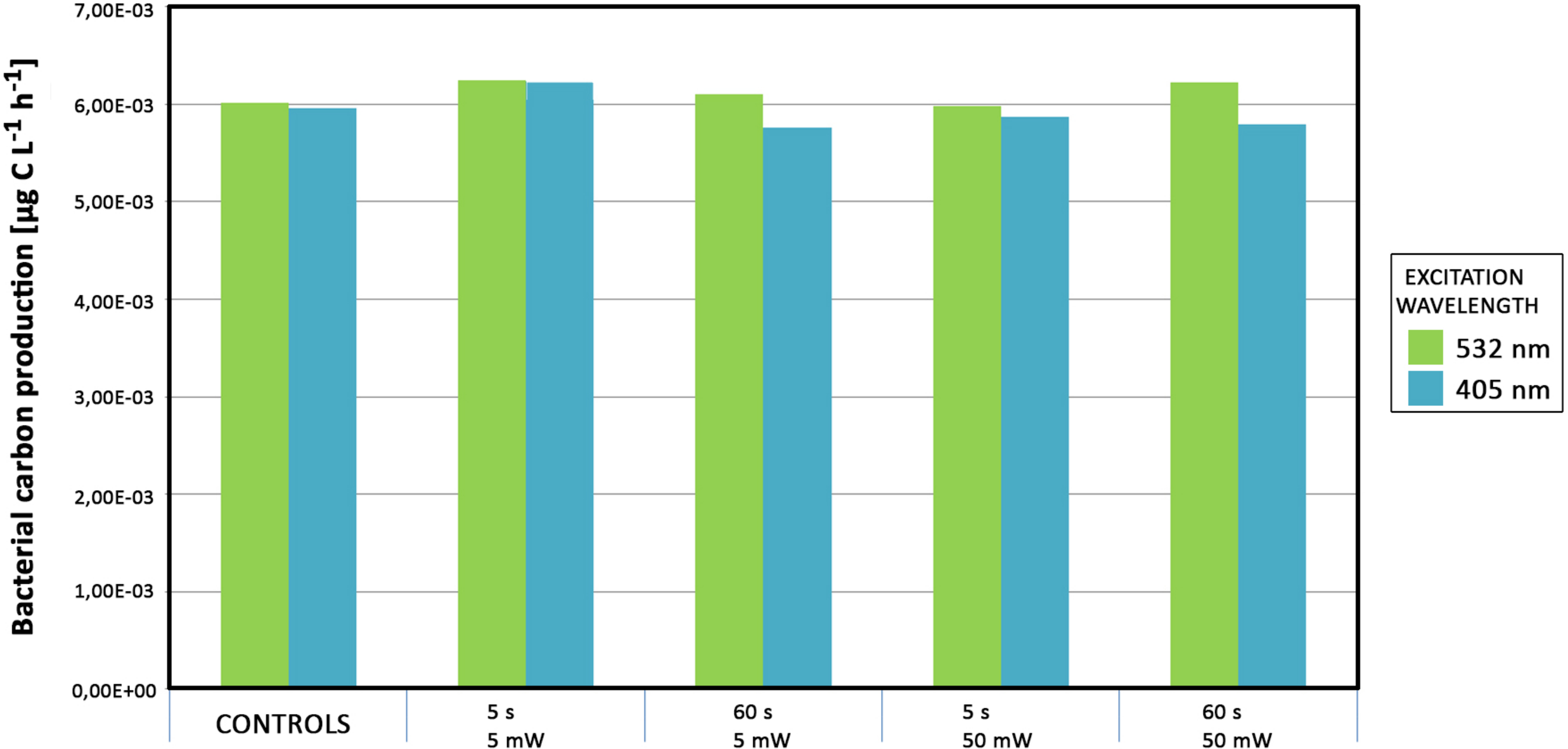

Figure

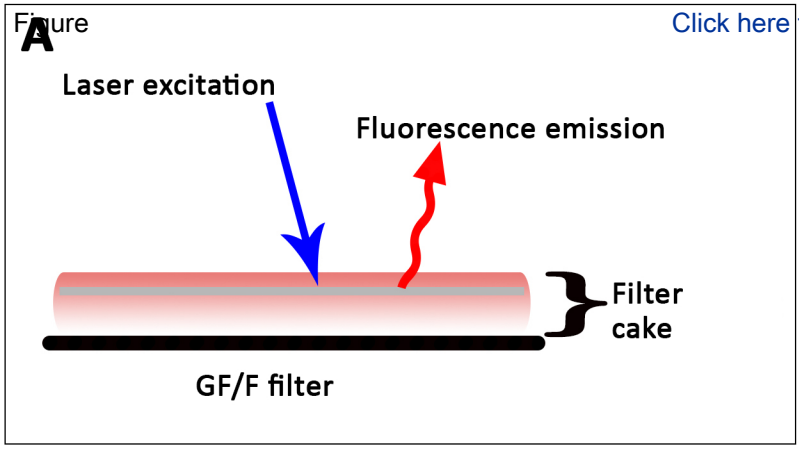

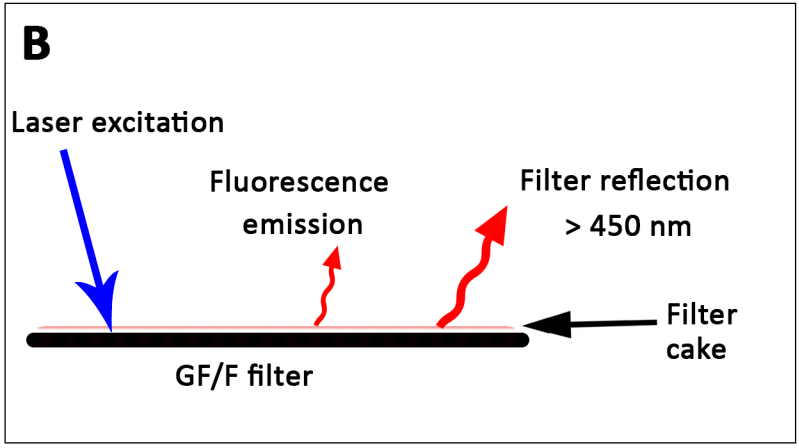

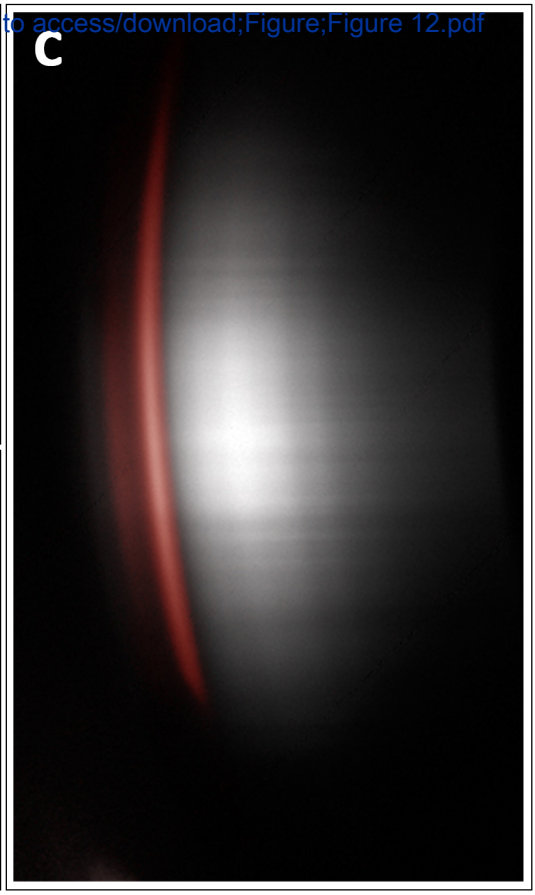

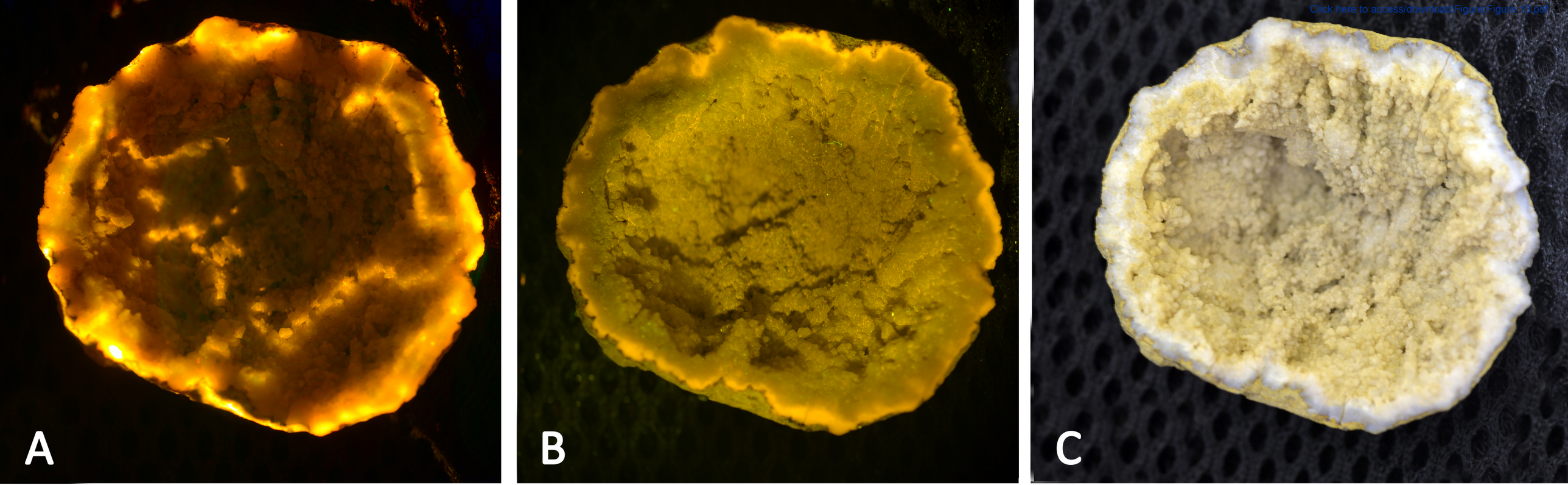

Figure

Click here to access/download;Figure;Figure 14.pdf

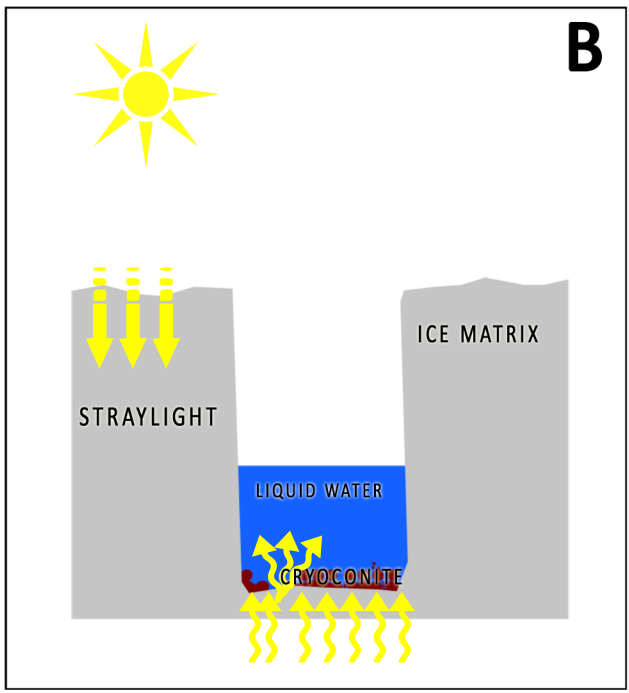

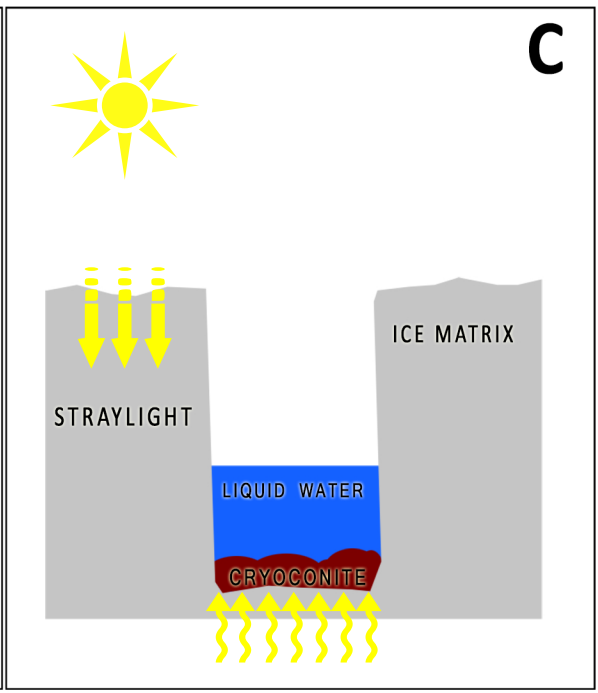

Table of Materials

Click here to access/download;Table of Materials;60447_R2_Weisleitner.xlsx

Name of Material/Equipment	Company	Catalog Number
aceton	Merck	67-64-1
B-Phycoerythrin	Invirtrogen	P6305
Chlorophyll a standard	Sigma-Aldrich	C6144-1MG
formaline	Merck	HT501128
GF/C filters	Whatman	WHA1822025
HCl	Merck	H1758
L.I.F.E. Prototype	University of Innsbruck	
LabView	National Instruments	
Leucine, L-[4,5-3H], 1 mCi	Perkin Elmer	NET1166001MC
Liquid scintillation cocktail Beckman Ready Us	Beckman	not more available, can be com
liquid scintillation counter	Beckman	out of stock
$NaH^{14}CO_3$ (4 µCi/ml)	DHI Denmark	4 µCi/ml, 1 ml
Osmonics polycarbonate filters	DHI Denmark	PCTE
Polyscintillation vials	Perkin Elmer	WHA1825047
sample tubes	Sigma Aldrich	T2318-500EA
Spectrophotometer	Hitachi	NA
trichloric acetic acid (TCA)	Merck	T6399
ultrasonic probe	nano lab	QS1T-2

Comments/Description

36%
25mm diameter
36,5-38%
built on demand
Software, Laboratory Virtual Instrumentation Engineering Workbench
radioactive
pensated by Ultra Gold, Packard
LSC 6000 IC
radioactive
25mm diameter, 0,2µm pore size
20ml
Greiner centrifuge tubes, 50ml
Model U2001, any photometer for absorption spectroscopy measuring at 664nm and 750nm would be appropria
100%

ate

jove JOURNAL OF VISUALIZED EXPERIMENTS
1 Alewife Center #200
Cambridge, MA 02140
tel. 617.945.9051
www.jove.com

ARTICLE AND VIDEO LICENSE AGREEMENT

Title of Article:	Laser Induced Fluorescence Emission (L.I.F.E.) as novel non-invasive tool for in-situ measaurements: calibration and application of a prototype
Author(s):	Weisleitner K., Hunger L., Kohstall C., Frisch A., Storrie-Lombardi M. and Sattler B.

Item 1: The Author elects to have the Materials be made available (as described at http://www.jove.com/publish) via:

☐ Standard Access ☒ Open Access

Item 2: Please select one of the following items:

☒ The Author is **NOT** a United States government employee.

☐ The Author is a United States government employee and the Materials were prepared in the course of his or her duties as a United States government employee.

☐ The Author is a United States government employee but the Materials were NOT prepared in the course of his or her duties as a United States government employee.

ARTICLE AND VIDEO LICENSE AGREEMENT

1. **Defined Terms.** As used in this Article and Video License Agreement, the following terms shall have the following meanings: "**Agreement**" means this Article and Video License Agreement; "**Article**" means the article specified on the last page of this Agreement, including any associated materials such as texts, figures, tables, artwork, abstracts, or summaries contained therein; "**Author**" means the author who is a signatory to this Agreement; "**Collective Work**" means a work, such as a periodical issue, anthology or encyclopedia, in which the Materials in their entirety in unmodified form, along with a number of other contributions, constituting separate and independent works in themselves, are assembled into a collective whole; "**CRC License**" means the Creative Commons Attribution-Non Commercial-No Derivs 3.0 Unported Agreement, the terms and conditions of which can be found at: http://creativecommons.org/licenses/by-nc-nd/3.0/legalcode; "**Derivative Work**" means a work based upon the Materials or upon the Materials and other pre-existing works, such as a translation, musical arrangement, dramatization, fictionalization, motion picture version, sound recording, art reproduction, abridgment, condensation, or any other form in which the Materials may be recast, transformed, or adapted; "**Institution**" means the institution, listed on the last page of this Agreement, by which the Author was employed at the time of the creation of the Materials; "**JoVE**" means MyJove Corporation, a Massachusetts corporation and the publisher of The Journal of Visualized Experiments; "**Materials**" means the Article and / or the Video; "**Parties**" means the Author and JoVE; "**Video**" means any video(s) made by the Author, alone or in conjunction with any other parties, or by JoVE or its affiliates or agents, individually or in collaboration with the Author or any other parties, incorporating all or any portion of the Article, and in which the Author may or may not appear.

2. **Background.** The Author, who is the author of the Article, in order to ensure the dissemination and protection of the Article, desires to have the JoVE publish the Article and create and transmit videos based on the Article. In furtherance of such goals, the Parties desire to memorialize in this Agreement the respective rights of each Party in and to the Article and the Video.

3. **Grant of Rights in Article.** In consideration of JoVE agreeing to publish the Article, the Author hereby grants to JoVE, subject to **Sections 4** and **7** below, the exclusive, royalty-free, perpetual (for the full term of copyright in the Article, including any extensions thereto) license (a) to publish, reproduce, distribute, display and store the Article in all forms, formats and media whether now known or hereafter developed (including without limitation in print, digital and electronic form) throughout the world, (b) to translate the Article into other languages, create adaptations, summaries or extracts of the Article or other Derivative Works (including, without limitation, the Video) or Collective Works based on all or any portion of the Article and exercise all of the rights set forth in (a) above in such translations, adaptations, summaries, extracts, Derivative Works or Collective Works and(c) to license others to do any or all of the above. The foregoing rights may be exercised in all media and formats, whether now known or hereafter devised, and include the right to make such modifications as are technically necessary to exercise the rights in other media and formats. If the "Open Access" box has been checked in **Item 1** above, JoVE and the Author hereby grant to the public all such rights in the Article as provided in, but subject to all limitations and requirements set forth in, the CRC License.

4. **Retention of Rights in Article.** Notwithstanding the exclusive license granted to JoVE in **Section 3** above, the Author shall, with respect to the Article, retain the non-exclusive right to use all or part of the Article for the non-commercial purpose of giving lectures, presentations or teaching classes, and to post a copy of the Article on the Institution's website or the Author's personal website, in each case provided that a link to the Article on the JoVE website is provided and notice of JoVE's copyright in the Article is included. All non-copyright intellectual property rights in and to the Article, such as patent rights, shall remain with the Author.

5. **Grant of Rights in Video – Standard Access.** This **Section 5** applies if the "Standard Access" box has been checked in **Item 1** above or if no box has been checked in **Item 1** above. In consideration of JoVE agreeing to produce, display or otherwise assist with the Video, the Author hereby acknowledges and agrees that, Subject to **Section 7** below, JoVE is and shall be the sole and exclusive owner of all rights of any nature, including, without limitation, all copyrights, in and to the Video. To the extent that, by law, the Author is deemed, now or at any time in the future, to have any rights of any nature in or to the Video, the Author hereby disclaims all such rights and transfers all such rights to JoVE.

6. **Grant of Rights in Video – Open Access.** This **Section 6** applies only if the "Open Access" box has been checked in **Item 1** above. In consideration of JoVE agreeing to produce, display or otherwise assist with the Video, the Author hereby grants to JoVE, subject to **Section 7** below, the exclusive, royalty-free, perpetual (for the full term of copyright in the Article, including any extensions thereto) license (a) to publish, reproduce, distribute, display and store the Video in all forms, formats and media whether now known or hereafter developed (including without limitation in print, digital and electronic form) throughout the world, (b) to translate the Video into other languages, create adaptations, summaries or extracts of the Video or other Derivative Works or Collective Works based on all or any portion of the Video and exercise all of the rights set forth in (a) above in such translations, adaptations, summaries, extracts, Derivative Works or Collective Works and (c) to license others to do any or all of the above. The foregoing rights may be exercised in all media and formats, whether now known or hereafter devised, and include the right to make such modifications as are technically necessary to exercise the rights in other media and formats. For any Video to which this **Section 6** is applicable, JoVE and the Author hereby grant to the public all such rights in the Video as provided in, but subject to all limitations and requirements set forth in, the CRC License.

7. **Government Employees.** If the Author is a United States government employee and the Article was prepared in the course of his or her duties as a United States government employee, as indicated in **Item 2** above, and any of the licenses or grants granted by the Author hereunder exceed the scope of the 17 U.S.C. 403, then the rights granted hereunder shall be limited to the maximum rights permitted under such statute. In such case, all provisions contained herein that are not in conflict with such statute shall remain in full force and effect, and all provisions contained herein that do so conflict shall be deemed to be amended so as to provide to JoVE the maximum rights permissible within such statute.

8. **Protection of the Work.** The Author(s) authorize JoVE to take steps in the Author(s) name and on their behalf if JoVE believes some third party could be infringing or might infringe the copyright of either the Author's Article and/or Video.

9. **Likeness, Privacy, Personality.** The Author hereby grants JoVE the right to use the Author's name, voice, likeness, picture, photograph, image, biography and performance in any way, commercial or otherwise, in connection with the Materials and the sale, promotion and distribution thereof. The Author hereby waives any and all rights he or she may have, relating to his or her appearance in the Video or otherwise relating to the Materials, under all applicable privacy, likeness, personality or similar laws.

10. **Author Warranties.** The Author represents and warrants that the Article is original, that it has not been published, that the copyright interest is owned by the Author (or, if more than one author is listed at the beginning of this Agreement, by such authors collectively) and has not been assigned, licensed, or otherwise transferred to any other party. The Author represents and warrants that the author(s) listed at the top of this Agreement are the only authors of the Materials. If more than one author is listed at the top of this Agreement and if any such author has not entered into a separate Article and Video License Agreement with JoVE relating to the Materials, the Author represents and warrants that the Author has been authorized by each of the other such authors to execute this Agreement on his or her behalf and to bind him or her with respect to the terms of this Agreement as if each of them had been a party hereto as an Author. The Author warrants that the use, reproduction, distribution, public or private performance or display, and/or modification of all or any portion of the Materials does not and will not violate, infringe and/or misappropriate the patent, trademark, intellectual property or other rights of any third party. The Author represents and warrants that it has and will continue to comply with all government, institutional and other regulations, including, without limitation all institutional, laboratory, hospital, ethical, human and animal treatment, privacy, and all other rules, regulations, laws, procedures or guidelines, applicable to the Materials, and that all research involving human and animal subjects has been approved by the Author's relevant institutional review board.

11. **JoVE Discretion.** If the Author requests the assistance of JoVE in producing the Video in the Author's facility, the Author shall ensure that the presence of JoVE employees, agents or independent contractors is in accordance with the relevant regulations of the Author's institution. If more than one author is listed at the beginning of this Agreement, JoVE may, in its sole

jove JOURNAL OF VISUALIZED EXPERIMENTS
1 Alewife Center #200
Cambridge, MA 02140
tel. 617.945.9051
www.jove.com

ARTICLE AND VIDEO LICENSE AGREEMENT

discretion, elect not take any action with respect to the Article until such time as it has received complete, executed Article and Video License Agreements from each such author. JoVE reserves the right, in its absolute and sole discretion and without giving any reason therefore, to accept or decline any work submitted to JoVE. JoVE and its employees, agents and independent contractors shall have full, unfettered access to the facilities of the Author or of the Author's institution as necessary to make the Video, whether actually published or not. JoVE has sole discretion as to the method of making and publishing the Materials, including, without limitation, to all decisions regarding editing, lighting, filming, timing of publication, if any, length, quality, content and the like.

12. **Indemnification.** The Author agrees to indemnify JoVE and/or its successors and assigns from and against any and all claims, costs, and expenses, including attorney's fees, arising out of any breach of any warranty or other representations contained herein. The Author further agrees to indemnify and hold harmless JoVE from and against any and all claims, costs, and expenses, including attorney's fees, resulting from the breach by the Author of any representation or warranty contained herein or from allegations or instances of violation of intellectual property rights, damage to the Author's or the Author's institution's facilities, fraud, libel, defamation, research, equipment, experiments, property damage, personal injury, violations of institutional, laboratory, hospital, ethical, human and animal treatment, privacy or other rules, regulations, laws, procedures or guidelines, liabilities and other losses or damages related in any way to the submission of work to JoVE, making of videos by JoVE, or publication in JoVE or elsewhere by JoVE. The Author shall be responsible for, and shall hold JoVE harmless from, damages caused by lack of sterilization, lack of cleanliness or by contamination due to the making of a video by JoVE its employees, agents or independent contractors. All sterilization, cleanliness or decontamination procedures shall be solely the responsibility of the Author and shall be undertaken at the Author's expense. All indemnifications provided herein shall include JoVE's attorney's fees and costs related to said losses or damages. Such indemnification and holding harmless shall include such losses or damages incurred by, or in connection with, acts or omissions of JoVE, its employees, agents or independent contractors.

13. **Fees.** To cover the cost incurred for publication, JoVE must receive payment before production and publication of the Materials. Payment is due in 21 days of invoice. Should the Materials not be published due to an editorial or production decision, these funds will be returned to the Author. Withdrawal by the Author of any submitted Materials after final peer review approval will result in a US$1,200 fee to cover pre-production expenses incurred by JoVE. If payment is not received by the completion of filming, production and publication of the Materials will be suspended until payment is received.

14. **Transfer, Governing Law.** This Agreement may be assigned by JoVE and shall inure to the benefits of any of JoVE's successors and assignees. This Agreement shall be governed and construed by the internal laws of the Commonwealth of Massachusetts without giving effect to any conflict of law provision thereunder. This Agreement may be executed in counterparts, each of which shall be deemed an original, but all of which together shall be deemed to me one and the same agreement. A signed copy of this Agreement delivered by facsimile, e-mail or other means of electronic transmission shall be deemed to have the same legal effect as delivery of an original signed copy of this Agreement.

A signed copy of this document must be sent with all new submissions. Only one Agreement is required per submission.

CORRESPONDING AUTHOR

Name:	Birgit Sattler
Department:	Institute of Ecology, Austrian Polar Research Institute
Institution:	University of Innsbruck
Title:	Ao. Univ.-Prof. Dr.
Signature:	
Date:	19.6.2019

Please submit a **signed** and **dated** copy of this license by one of the following three methods:

1. Upload an electronic version on the JoVE submission site
2. Fax the document to +1.866.381.2236
3. Mail the document to JoVE / Attn: JoVE Editorial / 1 Alewife Center #200 / Cambridge, MA 02140

Institute of Ecology
Leopold-Franzens-Universität Innsbruck
Technikerstraße 25 / AT - 6020 Innsbruck
Birgit Sattler, Ao. Univ.-Prof. Dr.
Austrian Polar Research Institute

Innsbruck, 12. September 2019

REBUTTAL LETTER

Weisleitner et al., JoVE 60447R1, LASER-INDUCED FLUORESCENCE EMISSION (L.I.F.E.) AS NOVEL NON-INVASIVE TOOL FOR IN-SITU MEASUREMENTS OF BIOMARKERS IN CRYOSPHERIC HABITATS

Dear Dr. Upponi,

dear Dr. Cao,

Once again, we would like to express our gratitude for your thorough revision of our manuscript and video which we hope is now in best shape.

We have gone through your issues point by point and have addressed every single one. All editorial concerns have been corrected and checked, the most critical was the slight inconsistency between the narrative in the video and the manuscript which has been solved now. It should read now along the video in a concomitant manner. Some issues regarding the voice with transitions and wordings have been corrected as well, however, due to the unavailability of our speaker, we had limited options but we hope that it fulfills all the requirements now.

There is a lot of lifeblood now in this publication and we very much hope that we could fulfill now your expectations and are very much looking forward to receiving a positive feedback.

Sincerely,

Ao.Univ.-Prof. Dr. Birgit Sattler

Institute of Ecology, Technikerstraße 25, A-6020 Innsbruck
Tel. +43 (0)512 507-51731 Fax +43 (0)512 507-51799 E-Mail: ecology@uibk.ac.at http://www.uibk.ac.at/ecology